

Orthogonal Actuation of a Supramolecular Double-Porphyrin Tweezer

Michael Schmittel* and Soumen K. Samanta

Center for Micro- and Nanochemistry and Engineering, Organische Chemie I, Adolf-Reichwein Str.,
Universität Siegen, D-57068 Siegen, Germany

schmittel@chemie.uni-siegen.de

Received June 15, 2010



A supramolecular three-component double-porphyrin tweezer (**PT**) is prepared quantitatively using heteroleptic complex formation along the HETTAP methodology. Insertion of guest molecules, such as DABCO or pyrazine, into the coupled porphyrin cavities of **PT** leads to an actuation of the double-porphyrin tweezer function. Evidence from ^1H NMR, VT NMR, and UV–vis titration suggests a rapid association/dissociation of the DABCO molecules at the central porphyrin. Upon addition of an equimolar mixture of DABCO and pyrazine to **PT**, a dynamic five-component self-assembled structure was furnished exclusively. ^1H NMR and K_{assoc} values validate the greater stability of the heteroloated **PT**-(DABCO)(py) system in comparison to the two homoloated systems, **PT**-(DABCO) $_2$ and **PT**-(py) $_2$. The higher stability of **PT**-(DABCO)(py) seems to be the result of charge transfer from DABCO to the vacant π^* orbital of pyrazine across the porphyrin plane.

Introduction

The rational design and fabrication of supramolecular nanoarchitectures of high structural diversity¹ and functionality² has received ample attention over recent years, in particular due to interesting emergent properties arising from electronic and optical interactions of individual components.

However, a growing number of components not only opens a venue for expanding emergence but also equally augments the complexity of all competing interactions in such a way that supramolecular self-assembly of multiple building blocks into a single species becomes increasingly demanding.^{1a} It thus comes as no surprise that, for example, the majority of all known metallosupramolecular aggregates consists of just one type of ligand and one sort of metal ion,³ whereas architectures with multiple ligands ($n \geq 2$) and multiple metal ions ($n \geq 2$) are found to be scarce.^{1f,4}

- (1) (a) De, S.; Mahata, K.; Schmittel, M. *Chem. Soc. Rev.* **2010**, 39, 1555. (b) Wang, M.; Zheng, Y.-R.; Ghosh, K.; Stang, P. J. *J. Am. Chem. Soc.* **2010**, 132, 6282. (c) Mal, P.; Nitschke, J. R. *Chem. Commun.* **2010**, 46, 2417. (d) Northrop, B. H.; Zheng, Y.-R.; Chi, K.-W.; Stang, P. J. *Acc. Chem. Res.* **2009**, 42, 1554. (e) Klosterman, J. K.; Yamauchi, Y.; Fujita, M. *Chem. Soc. Rev.* **2009**, 38, 1714. (f) Schmittel, M.; Mahata, K. *Angew. Chem., Int. Ed.* **2008**, 47, 5284. (g) Nitschke, J. R. *Acc. Chem. Res.* **2007**, 40, 103. (h) Schmittel, M.; Kalsani, V.; Michel, C.; Mal, P.; Ammon, H.; Jäckel, F.; Rabe, J. P. *Chem.—Eur. J.* **2007**, 13, 6223. (i) Fiedler, D.; Leung, D. H.; Bergman, R. G.; Raymond, K. N. *Acc. Chem. Res.* **2005**, 38, 351. (j) Fujita, M.; Tominaga, M.; Hori, A.; Therrien, B. *Acc. Chem. Res.* **2005**, 38, 371. (k) Fujita, M. *Chem. Soc. Rev.* **1998**, 27, 417. (2) (a) Sawada, T.; Fujita, M. *J. Am. Chem. Soc.* **2010**, 132, 7194. (b) Brown, C. J.; Bergman, R. G.; Raymond, K. N. *J. Am. Chem. Soc.* **2009**, 131, 17530. (c) Yoshizawa, M.; Klosterman, J. K.; Fujita, M. *Angew. Chem., Int. Ed.* **2009**, 48, 3418. (d) Northrop, B. H.; Yang, H.-B.; Stang, P. J. *Chem. Commun.* **2008**, 5896. (e) Schmittel, M.; Kishore, R. S. K.; Bats, J. W. *Org. Biomol. Chem.* **2007**, 5, 78. (f) Grozema, F. C.; Houarner-Rassin, C.; Prins, P.; Siebbeles, L. D. A.; Anderson, H. L. *J. Am. Chem. Soc.* **2007**, 129, 13370. (g) Würthner, F.; You, C. C.; Saha-Möller, C. R. *Chem. Soc. Rev.* **2004**, 33, 133. (h) Screen, T. E. O.; Thorne, G. R. G.; Denning, R. G.; Bucknall, D. G.; Anderson, H. L. *J. Am. Chem. Soc.* **2002**, 124, 9712.

- (3) (a) Tominaga, M.; Suzuki, K.; Kawano, M.; Kusukawa, T.; Ozeki, T.; Sakamoto, S.; Yamaguchi, K.; Fujita, M. *Angew. Chem., Int. Ed.* **2004**, 43, 5621. (b) Hwang, I.-W.; Kamada, T.; Ahn, T. K.; Ko, D. M.; Nakamura, T.; Tsuda, A.; Osuka, A.; Kim, D. *J. Am. Chem. Soc.* **2004**, 126, 16187. (c) Drain, C. M.; Batteas, J. M.; Flynn, G. W.; Milic, T.; Chi, N.; Yablon, D. G.; Sommers, H. *Proc. Natl. Acad. Sci. U.S.A.* **2002**, 99, 6498. (d) Davis, A. V.; Yeh, R. M.; Raymond, K. N. *Proc. Natl. Acad. Sci. U.S.A.* **2002**, 99, 4793. (e) Jolliffe, K. A.; Timmerman, P.; Reinhoudt, D. N. *Angew. Chem., Int. Ed.* **1999**, 38, 933. (f) Fujita, M. *Acc. Chem. Res.* **1999**, 32, 53. (4) (a) Mahata, K.; Schmittel, M. *J. Am. Chem. Soc.* **2009**, 131, 16545. (b) Christinat, N.; Scopelliti, R.; Severin, K. *Angew. Chem., Int. Ed.* **2008**, 47, 1848. (c) Liu, Y.; Bruneau, A.; He, J.; Abliz, Z. *Org. Lett.* **2008**, 10, 765. (d) Pentecost, C. D.; Chichak, K. S.; Peters, A. J.; Cave, G. W. V.; Cantrill, S. J.; Stoddart, J. F. *Angew. Chem., Int. Ed.* **2007**, 46, 218. (e) Guo, X.; Whalley, A.; Klare, J. E.; Huang, L.; O'Brien, S.; Steigerwald, M.; Nuckolls, C. *Nano Lett.* **2007**, 7, 1119. (f) Kishore, R. S. K.; Paululat, T.; Schmittel, M. *Chem.—Eur. J.* **2006**, 12, 8136. (g) Kumazawa, K.; Biradha, K.; Kusukawa, T.; Okano, T.; Fujita, M. *Angew. Chem., Int. Ed.* **2003**, 42, 3909.

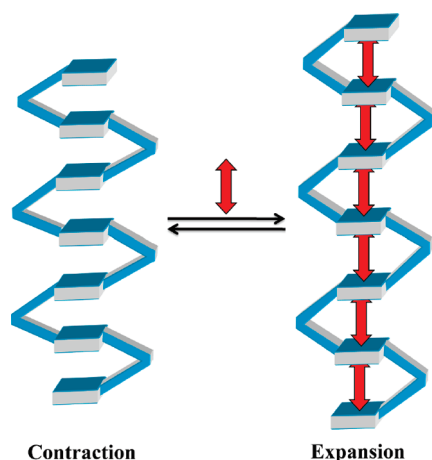


FIGURE 1. Schematic diagram of the accordion and its reversible expansion and contraction as a function of chemical additives.

The fabrication of a multicomponent aggregate as a single species under thermodynamic equilibrium conditions requires instilling either a fully orthogonal or hierarchical self-assembly process and to precisely amalgamate all specific molecular binding preferences. Evidently, the viability of orthogonal binding algorithms can be evaluated by testing the noninterference of multiple reversible interactions,⁵ for example, in competitive self-sorting schemes.^{4a,6} At present, state-of-the-art multicomponent aggregates contain only five^{4a,7} different molecular components, and it is thus useful to further develop the tool box of new orthogonal interactions enriching the synthetic methodology of supramolecular chemistry.

Our work toward multicomponent systems was furthermore motivated by the keen prospect that amalgamation of multiple orthogonal noncovalent interactions allows one not only to forge static structures but also—if properly designed—to implement nanomechanical action⁸ into supramolecular assemblies. Along the latter line, we suggest building a supramolecular multiporphyrin accordion, the contraction and elongation of which may be controlled by chemical additives, as shown in a cartoon fashion in Figure 1. As a first step toward the development of supramolecular accordions, we present below the elaboration of a subunit of the supramolecular

accordion, which can be viewed as a three-component heteroleptic nanoscale double-porphyrin tweezer, and its actuation by chemical additives. While the preparation of the double-porphyrin tweezer is based on the formation of a heteroleptic terpyridine–phenanthroline complex along the HETTAP concept,⁹ the chemical actuators will operate via axial coordination in the zinc(II) porphyrin cavities. Notably, we will reveal that the actuation can even be triggered by a chemical signal $A + B$, which requires controlling the clean formation of a five-component assembly using noninterfering orthogonal binding algorithms under thermodynamic equilibrium conditions.

A prerequisite for a multiporphyrin accordion is a synthetic approach to a full or near cofacial arrangement of porphyrins, a motif well-known from light harvesting and energy transfer studies.^{10,11} Although considerable attempts have been taken to prepare highly preorganized multiporphyrin systems, a large amount of studies makes use of the covalent approach.¹² The more ambitious and adaptable strategy is, however, to build such functional structures by a faultless self-assembly process.¹³

An exciting feature of zinc porphyrins is their ability to readily bind a variety of ligands at the axial coordination site.^{13,14} However, due to the d^{10} electronic configuration of the zinc(II) and the enforced square-planar coordination by the porphyrin, zinc porphyrins usually do not embrace two axial ligands simultaneously. Rather, the binding of the sixth ligand to the Zn^{2+} center weakens the binding of the fifth ligand thermodynamically and kinetically.^{4f,15} While a good number of di- and oligoporphyrin architectures (mostly with an even number of porphyrins) have been used as hosts for the recognition of guest molecules,¹⁶ the selective trapping of

- (5) (a) Lee, J.; Ghosh, K.; Stang, P. J. *J. Am. Chem. Soc.* **2009**, *131*, 12028. (b) Ajami, D.; Rebek, J., Jr. *J. Org. Chem.* **2009**, *74*, 6584. (c) Chas, M.; Blanco, V.; Peinador, C.; Quintela, J. M. *Org. Lett.* **2007**, *9*, 675. (d) Kishore, R. S. K.; Kalsani, V.; Schmittel, M. *Chem. Commun.* **2006**, 3690. (e) Chichak, K. S.; Cantrill, S. J.; Pease, A. R.; Chiu, A.-H.; Cave, G. W. V.; Atwood, J. L.; Stoddart, J. F. *Science* **2004**, *304*, 1308. (f) Stulz, E.; Ng, Y.-F.; Scott, S. M.; Sanders, J. K. M. *Chem. Commun.* **2002**, 524.
- (6) (a) Schmittel, M.; Mahata, K. *Chem. Commun.* **2010**, 46, 4163. (b) Jiang, W.; Schalley, C. A. *Proc. Natl. Acad. Sci. U.S.A.* **2009**, *106*, 10425. (c) Wang, F.; Han, C.; He, C.; Zhou, C.; Wang, C.; Li, N.; Huang, F. *J. Am. Chem. Soc.* **2008**, *130*, 11254. (d) Schultz, D.; Nitschke, J. R. *Angew. Chem., Int. Ed.* **2006**, *45*, 2453. (e) Lehn, J.-M. *Science* **2002**, *295*, 2400. (f) Krämer, R.; Lehn, J.-M.; Marquis-Rigault, A. *Proc. Natl. Acad. Sci. U.S.A.* **1993**, *90*, 5394.
- (7) Murase, T.; Otsuka, K.; Fujita, M. *J. Am. Chem. Soc.* **2010**, *132*, 7864.
- (8) (a) Miwa, K.; Furusho, Y.; Yashima, E. *Nat. Chem.* **2010**, *2*, 444. (b) Chuang, C.-J.; Li, W.-S.; Lai, C.-C.; Liu, Y.-H.; Peng, S.-M.; Chao, I.; Chiu, S.-H. *Org. Lett.* **2009**, *11*, 385. (c) Dawson, R. E.; Lincoln, S. F.; Easton, C. J. *Chem. Commun.* **2008**, 3980. (d) Saha, S.; Flood, A. H.; Stoddart, J. F.; Impellizzeri, S.; Silvi, S.; Venturi, M.; Credi, A. *J. Am. Chem. Soc.* **2007**, *129*, 12159. (e) Liu, Y.; Flood, A. H.; Bonvallet, P. A.; Vignon, S. A.; Northrop, B. H.; Tseng, H.-R.; Jeppesen, J. O.; Huang, T. J.; Brough, B.; Baller, M.; Magonov, S.; Solares, S. D.; Goddard, W. A.; Ho, C.-M.; Stoddart, J. F. *J. Am. Chem. Soc.* **2005**, *127*, 9745. (f) Sauvage, J.-P. *Chem. Commun.* **2005**, 1507. (g) Collin, J.-P.; Dietrich-Buchecker, C.; Gavina, P.; Jimenez-Molero; Sauvage, J.-P. *Acc. Chem. Res.* **2001**, *34*, 477.

- (9) (a) Schmittel, M.; Mahata, K. *Inorg. Chem.* **2009**, *48*, 822. (b) Schmittel, M.; Kalsani, V.; Mal, P.; Bats, J. W. *Inorg. Chem.* **2006**, *45*, 6370. (c) Schmittel, M.; Kalsani, V.; Kishore, R. S. K.; Cölfen, H.; Bats, J. W. *J. Am. Chem. Soc.* **2005**, *127*, 11544.
- (10) (a) Yamamura, T.; Suzuki, S.; Taguchi, T.; Onoda, A.; Kamachi, T.; Okura, I. *J. Am. Chem. Soc.* **2009**, *131*, 11719. (b) Kuramochi, Y.; Sandanayaka, A. S. D.; Satake, A.; Araki, Y.; Ogawa, K.; Ito, O.; Kobuke, Y. *Chem.—Eur. J.* **2009**, *15*, 2317. (c) D'Souza, F.; Chitta, R.; Gadde, S.; Rogers, L. M.; Karr, P. A.; Zandler, M. E.; Sandanayaka, A. S. D.; Araki, Y.; Ito, O. *Chem.—Eur. J.* **2007**, *13*, 916. (d) Haycock, R. A.; Yartsev, A.; Michelsen, U.; Sundström, V.; Hunter, C. A. *Angew. Chem., Int. Ed.* **2000**, *39*, 3616.
- (11) (a) Faure, S.; Stern, C.; Guillard, R.; Harvey, P. D. *J. Am. Chem. Soc.* **2004**, *126*, 1253. (b) Holten, D.; Bocian, D. F.; Lindsey, J. S. *Acc. Chem. Res.* **2002**, *35*, 57–69. (c) Hunter, C. A.; Hyde, R. K. *Angew. Chem., Int. Ed. Engl.* **1996**, *35*, 1936.
- (12) (a) Lee, D. C.; Morales, G. M.; Lee, Y.; Yu, L. *Chem. Commun.* **2006**, 100. (b) Kieran, A. L.; Pascu, S. I.; Jarroson, T.; Gunter, M. J.; Sanders, J. K. M. *Chem. Commun.* **2005**, 1842. (c) Shoji, O.; Okada, S.; Satake, A.; Kobuke, Y. *J. Am. Chem. Soc.* **2005**, *127*, 2201. (d) Shoji, O.; Tanaka, H.; Kawai, T.; Kobuke, Y. *J. Am. Chem. Soc.* **2005**, *127*, 8598. (e) Yagi, S.; Yonekura, I.; Awakura, M.; Ezoe, M.; Takagishi, T. *Chem. Commun.* **2001**, 557. (f) Tsuda, A.; Osuka, A. *Science* **2001**, *293*, 79.
- (13) (a) Beletskaya, I.; Tyurin, V. S.; Tsivadze, A. Y.; Guillard, R.; Stern, C. *Chem. Rev.* **2009**, *109*, 1659. (b) Drain, C. M.; Varotto, A.; Radivojevic, I. *Chem. Rev.* **2009**, *109*, 1630.
- (14) (a) Ballester, P.; Costa, A.; Castilla, A. M.; Deyà, P. M.; Frontera, A.; Gomila, R. M.; Hunter, C. A. *Chem.—Eur. J.* **2005**, *11*, 2196. (b) Ballester, P.; Costa, A.; Deyà, P. M.; Frontera, A.; Gomila, R. M.; Oliva, A. I.; Sanders, J. K. M.; Hunter, C. A. *J. Org. Chem.* **2005**, *70*, 6616. (c) Taylor, P. N.; Anderson, H. L. *J. Am. Chem. Soc.* **1999**, *121*, 11538. (d) Mak, C. C.; Bampas, N.; Sanders, J. K. M. *Angew. Chem., Int. Ed.* **1998**, *37*, 3020.
- (15) (a) Kleij, A. W.; Kuli, M.; Tooke, D. M.; Spek, A. L.; Reek, J. N. H. *Inorg. Chem.* **2005**, *44*, 7696. (b) Goldberg, I. *Chem.—Eur. J.* **2000**, *6*, 3863.
- (16) (a) Osswald, P.; You, C.-C.; Stepanenko, V.; Würthner, F. *Chem.—Eur. J.* **2010**, *15*, 2386. (b) Zahn, S.; Reckien, W.; Kircner, B.; Staats, H.; Matthey, J.; Lützen, A. *Chem.—Eur. J.* **2009**, *15*, 2572. (c) Darbost, U.; Sénéque, O.; Li, Y.; Bertho, G.; Marrot, J.; Rager, M.-N.; Renaud, O.; Jabin, I. *Chem.—Eur. J.* **2007**, *13*, 2078. (d) Kieran, A. L.; Pascu, S. I.; Jarroson, T.; Sanders, J. K. M. *Chem. Commun.* **2005**, 1276.

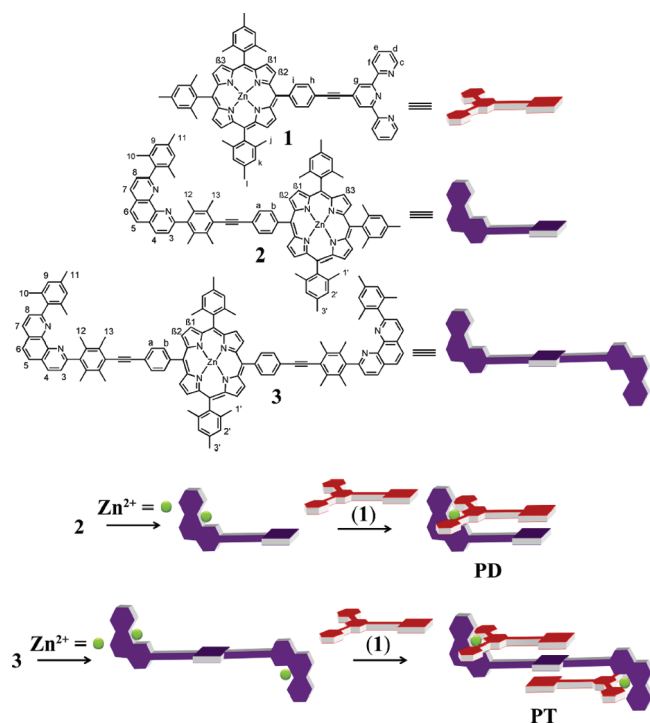


FIGURE 2. Ligands **1–3** used for the study (top) and a cartoon depiction of their self-assembly furnishing porphyrin tweezer **PD** and double tweezer **PT** (bottom).

heteroguest pairs remains a challenge, being hardly covered in the literature.¹⁷

Results and Discussion

Our approach to the porphyrin tweezer **PD** (a porphyrin “dimer”) and the coupled double-porphyrin tweezer **PT** (a porphyrin “trimer”) relies on the metallosupramolecular assembly of two organic components, as depicted in Figure 2, using the HETTAP methodology.⁹ Ligands **1–3**, required for the present study, were prepared by Sonogashira coupling protocols.¹⁸ Thus, zinc(II) 5-(4-iodophenyl)-10,15,20-tris(2,4,6-trimethylphenyl)porphyrin¹⁹ (**4**) was treated with 4'-ethynyl-2,2':6'2''-terpyridine (**5**) or 2-(4-ethynyl-2,3,5,6-tetramethylphenyl)-9-(2,4,6-trimethylphenyl)-[1,10]-phenanthroline (**6**) using Pd(PPh₃)₄ to afford **1** or **2** in 62 or 59% yield (Scheme 1). Using the same procedure, zinc(II) 5,15-bis(4-iodophenyl)-10,20-bis(2,4,6-trimethylphenyl)porphyrin^{19a,20} (**7**) was reacted with **6** to afford **3** in 55% yield (Scheme 1).

In line with earlier work,⁹ the HETTAP algorithm, implemented into ligands **1–3**, proved its high dependability and

robustness also in the present self-assembly processes, as demonstrated by the quantitative heteroleptic complex formation upon mixing of one of the phenanthroline-appended porphyrin ligands (**2** or **3**) with the terpyridine-appended porphyrin **1** in the presence of Zn(OTf)₂. The steric shielding of the bulky 2,9-diarylphenanthroline is imperative to prevent formation of any homoleptic^{1h,9,21} complex [M(PhenAr₂)₂]ⁿ⁺, with Mⁿ⁺ = Cu⁺, Ag⁺, Zn²⁺. As a consequence of maximum site occupancy effects,^{4a,6f,22} the PhenAr₂ ligand will combine with a sterically unassuming counterpart (e.g., terpyridine) in the presence of Mⁿ⁺ to furnish quantitatively the heteroleptic metal complex (HETTAP complex).⁹ As terpyridines typically form bishomoleptic complexes in the presence of many metal ions,²³ it is desirable to avoid formation of any unwanted homoleptic bisterpyridine complex right at the onset by combining all components sequentially. Consequently, **2** and Zn(OTf)₂ were first solubilized in acetonitrile/dichloromethane (3:1) prior to addition of **1**. Because of its low solubility, **1** was added to the mixture at 60 °C, affording the porphyrin dimer **PD** in quantitative yield after 3 h. Analogously, when compound **3** was combined with 2 equiv of **1** in the presence of Zn(OTf)₂ in the same solvent mixture, the porphyrin trimer **PT** formed in quantitative yield.

Both complexes **PD** and **PT** were characterized by ¹H NMR, ¹H–¹H COSY, ESI-MS, and elemental analysis. **PD** = [Zn(**1**)(**2**)]²⁺ displayed a characteristic upfield shift of the phenanthroline's mesityl C_{Ar}–H protons in **2** from 6.97 to 6.33 ppm in the ¹H NMR due to a shielding by the terpyridine π system of **1**, typical for any HETTAP complex.⁹ Analogously, in **PT** = [Zn(**1**)₂(**3**)]⁴⁺, the phenanthroline mesityl protons of **3** experienced an upfield shift from 6.96 to 6.30 ppm (Figure 3).⁹ Reciprocally, the α-protons of the terpyridines experienced a diagnostic upfield shift (from δ = 8.78 to 7.82 ppm). Furthermore, the phenanthroline 4,7-H and 3,8-H of both ligands **2** and **3** were shifted downfield to ca. 8.25 and 9.21 ppm, respectively, obviously due to metal complexation. As a consequence of porphyrin stacking, the C_{Ar}–H mesityl protons of the central porphyrin are shielded by the π electrons of the additional porphyrin unit(s); in **PD**, they show up at ca. 6.85 ppm and in **PT** at ca. 6.5 ppm. In the case of **PT**, the shielding is more enhanced because the central porphyrin unit is sandwiched between two porphyrins.

ESI-MS provided additionally conclusive evidence for the clean formation of the self-assembled **PD** and **PT**. The ESI-MS spectrum of **PD** displays a diagnostic peak at 1190.6 Da, representing **PD** after loss of two triflate counteranions [M – 2OTf]²⁺. The experimentally observed isotopic distribution agreed fully with the theoretical expectation. Analogous results were obtained for the self-assembled porphyrin trimer **PT** (Figure 3). The ESI-MS shows four diagnostic peaks after loss of triflate counteranions and fragmentation. The peaks at m/z = 979.4 and 1355.5 Da correspond to **PT** after loss of four and three triflate anions, respectively. The peaks at m/z = 1395.0 and 1464.5 Da correspond to [Zn(**1**)(**3**)]²⁺

(17) (a) Lee, C.-H.; Yoon, H.; Jang, W.-D. *Chem.—Eur. J.* **2009**, *15*, 9972. (b) Hwang, I.; Ziganshina, A. Y.; Ko, Y. H.; Yun, G.; Kim, K. *Chem. Commun.* **2009**, 416 and references therein. (c) Han, T.; Chen, C.-F. *Org. Lett.* **2007**, *9*, 4207. (d) Haino, T.; Kobayashi, M.; Chikaraishi, M.; Fukazawa, Y. *Chem. Commun.* **2005**, 2321. (e) Sato, H.; Tashiro, K.; Shinmori, H.; Osuka, A.; Murata, Y.; Komatsu, K.; Aida, T. *J. Am. Chem. Soc.* **2005**, *127*, 13086. (f) Yoshizawa, M.; Takeyama, T.; Okano, T.; Fujita, M. *J. Am. Chem. Soc.* **2003**, *125*, 3243.

(18) (a) Schmittel, M.; Michel, C.; Wiegrefe, A. *Synthesis* **2005**, *10*, 367. (b) de Meijere, A.; Meyer, F. E. *Angew. Chem., Int. Ed. Engl.* **1994**, *33*, 2379.

(19) (a) Wagner, R. W.; Johnson, T. E.; Lindsey, J. S. *J. Am. Chem. Soc.* **1996**, *118*, 11166. (b) Lindsey, J. S.; Prathapan, S.; Johnson, T. E.; Wagner, R. W. *Tetrahedron* **1994**, *50*, 8941.

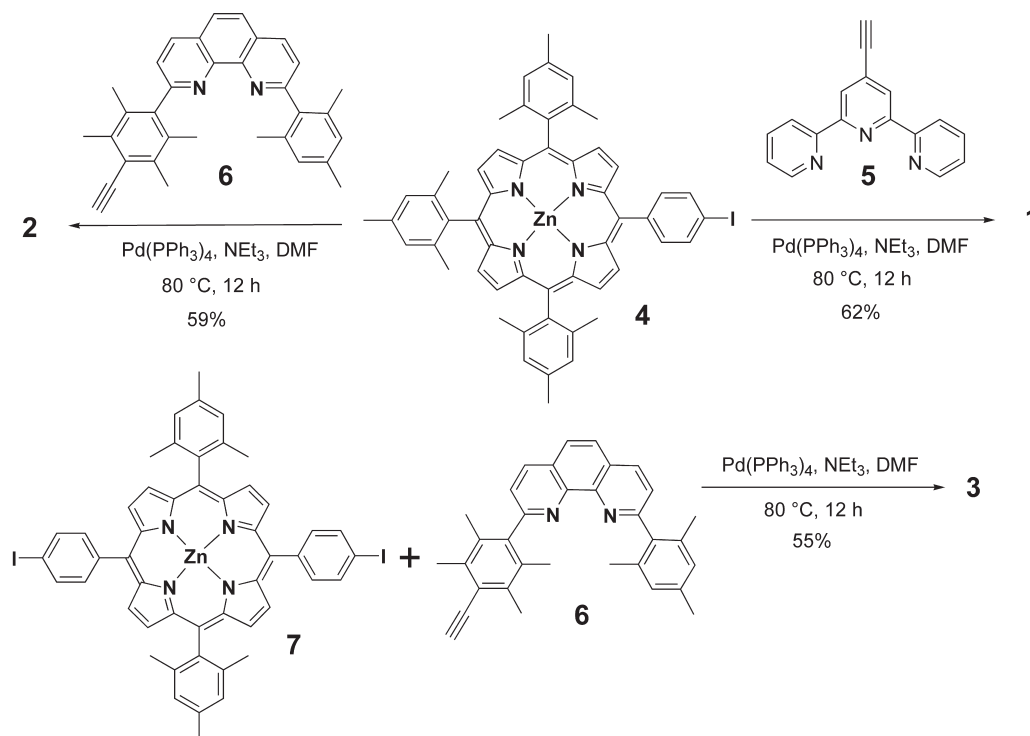
(20) (a) Littler, B. J.; Ciringh, Y.; Lindsey, J. S. *J. Org. Chem.* **1999**, *64*, 2864. (b) Lee, C.-H.; Lindsey, J. S. *Tetrahedron* **1994**, *50*, 11427.

(21) (a) Schmittel, M.; Mal, P. *Chem. Commun.* **2008**, 960. (b) Schmittel, M.; Ganz, A.; Fenske, D. *Org. Lett.* **2002**, *4*, 2289.

(22) (a) Fenton, H.; Tidmarsh, I. S.; Ward, M. D. *Dalton Trans.* **2009**, 4199. (b) Frey, J.; Tock, C.; Collin, J.-P.; Heitz, V.; Sauvage, J.-P.; Rissanen, K. *J. Am. Chem. Soc.* **2008**, *130*, 11013. (c) Sleiman, H.; Baxter, P.; Lehn, J.-M.; Rissanen, K. *J. Chem. Soc., Chem. Commun.* **1995**, 715.

(23) (a) Hofmeier, H.; Schubert, U. S. *Chem. Soc. Rev.* **2004**, *33*, 373. (b) Newkome, G. R.; Cho, T. J.; Moorefield, C. N.; Mohapatra, P. P.; Godinez, L. A. *Chem.—Eur. J.* **2004**, *10*, 1493.

SCHEME 1. Synthesis of Ligands 1, 2, and 3



and $[\text{ZnH}(\mathbf{1})(\mathbf{3})](\text{OTf})^{2+}$, respectively, and are thus expected fragments of **PT**. All peaks were isotopically well-resolved and agreed fully with the theoretical distribution. Finally, ^1H DOSY NMR confirmed the formation of both assemblies **PT** and **PD** in solution as single species.

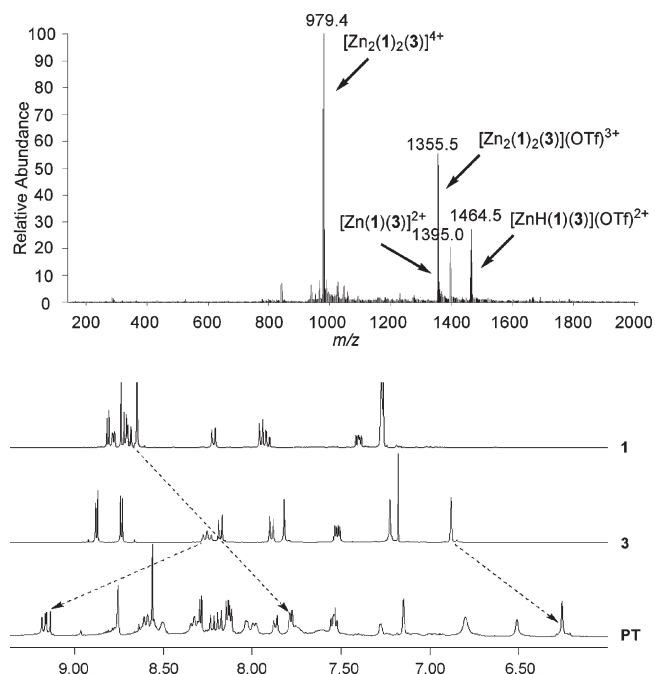


FIGURE 3. (Top) ESI-MS of **PT** in $\text{CH}_3\text{CN}/\text{CH}_2\text{Cl}_2$ (3:1). (Bottom) Partial ^1H NMR (400 MHz, 298 K) spectra of **1** (CDCl_3), **3** (CDCl_3), and **PT** (CD_3CN).

The MM+ force-field-computed structure of **PT** (Hyperchem) showed the porphyrin units to be aligned in a slipped cofacial

arrangement (Figure 4). Thus, all three porphyrins are arranged face-to-face with the central moiety being laterally shifted with respect to the two other porphyrins. Both **PD** and **PT** display a Pac-Man-type arrangement exhibiting a distance of 5.8 Å between two cofacial porphyrins. After complexation of DABCO into the tweezer subunit, a distance of 6.8 Å is

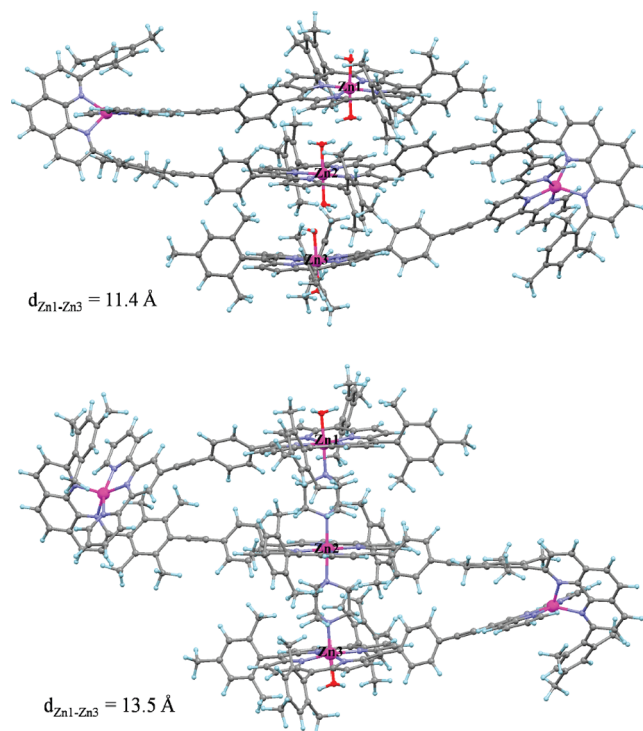


FIGURE 4. MM+ minimized structure of **PT** (top) and **PT-(DABCO)**₂ (bottom).

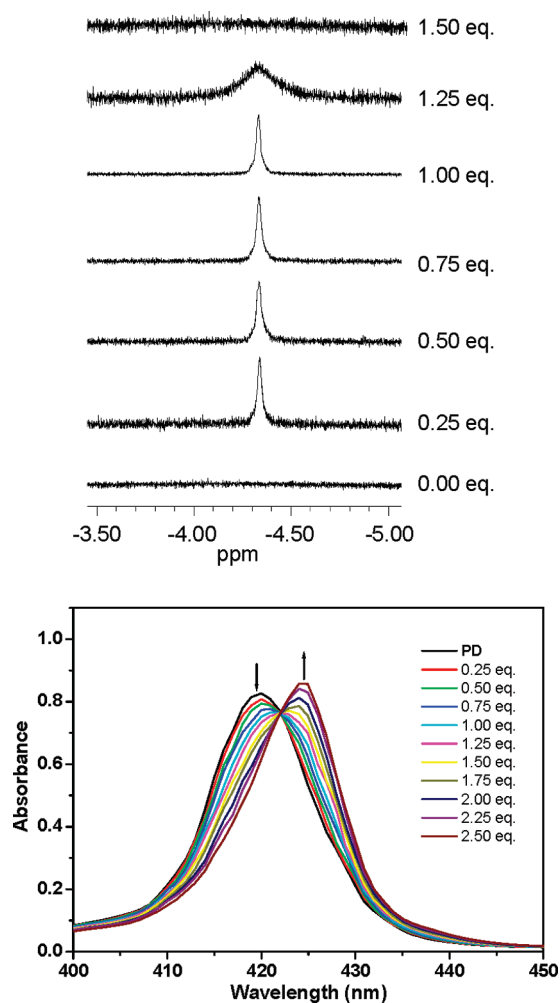


FIGURE 5. (Top) Evolution of ^1H NMR signals of DABCO at $25\text{ }^\circ\text{C}$ during titration of **PD** (0.47 mM) with DABCO in CD_2Cl_2 . (Bottom) UV-vis titration of **PD** ($0.97\text{ }\mu\text{M}$) with DABCO in CH_2Cl_2 at $25\text{ }^\circ\text{C}$.

realized between two neighboring porphyrins and one of $13.5\text{ }\text{\AA}$ between the two terminal porphyrins.

When **PD** was reacted with DABCO (1 equiv), a sharp singlet at -4.37 ppm (Figure 5), corresponding to the CH_2 protons of DABCO, indicated the formation of a **PD**-(DABCO) aggregate.²⁴ Upon addition of another 1 equiv of DABCO, the signal shifted from -4.37 to -3.2 ppm (very broad peak, not shown in Figure 5, top), indicating that bound and free DABCO were exchanging at room temperature. Notably, **PD**-(DABCO) was also detectable in the ESI-MS spectrum by a characteristic peak at 1247.3 Da , corresponding to the adduct after loss of two counteranions (OTf^-) (see Supporting Information). In line with earlier reports, the sandwich structure was confirmed by a 3 nm red shift of the Soret band upon addition of 1 equiv of DABCO, evidently attesting binding of DABCO in the bisporphyrin cavity of **PD**. Extra addition of DABCO resulted in a further bathochromic shift of the Soret band by 2 nm (Figure 5), indicating exchange of

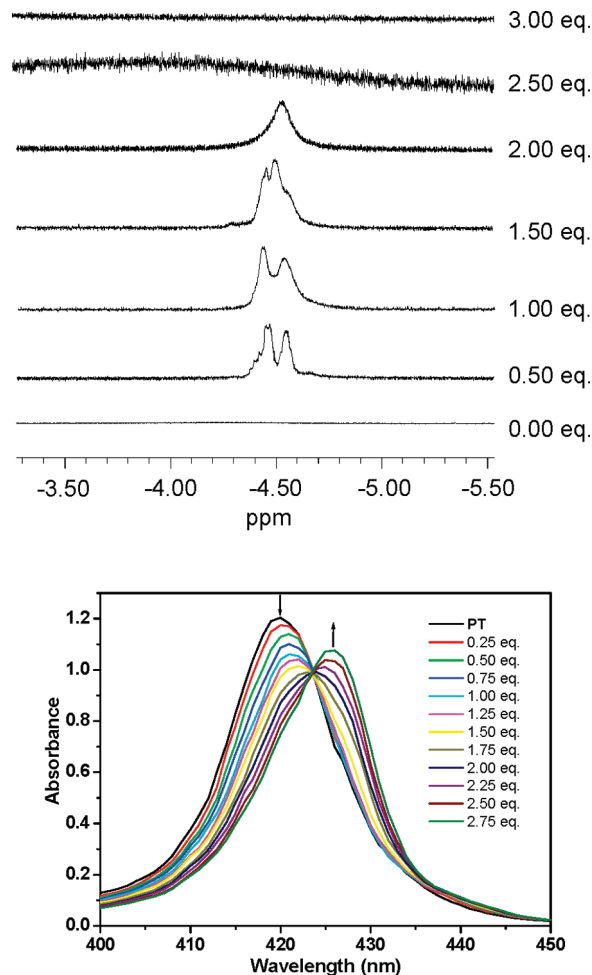


FIGURE 6. (Top) Evolution of ^1H NMR signals of DABCO at $25\text{ }^\circ\text{C}$ during titration of **PT** (0.57 mM) with DABCO in CD_2Cl_2 . (Bottom) UV-vis titration of **PT** ($1.54\text{ }\mu\text{M}$) with DABCO in CH_2Cl_2 at $25\text{ }^\circ\text{C}$.

free and bound DABCO. Further evidence for the formation of **PD**-(DABCO) can be inferred from the Job plot (UV-vis data) that indicated a 1:1 stoichiometry. The thermodynamic driving force,²⁵ as probed by a UV-vis titration, provided a K_{assoc} for **PD**-(DABCO) of $2.0 \times 10^8\text{ M}^{-1}$ ($\log K = 8.3 \pm 0.5$), a value at the high end in comparison to that of other bisporphyrinic tweezers²⁶ (for example, $2.02 \times 10^5\text{ M}^{-1}$).^{26b}

When **PT** was treated with DABCO in CD_2Cl_2 , the peak at $\delta = \text{ca. } -4.5\text{ ppm}$ was attributed to the formation of a single and a double sandwich complex.²⁴ Addition of 1 equiv of DABCO led to the appearance of two peaks ($\delta = -4.47$ and -4.55 ppm), which were not unexpected due to the chemically slightly nonequivalent porphyrin environment (Figure 6). Upon addition of a further 1 equiv of DABCO, the two

(24) (a) Ballester, P.; Oliva, A. I.; Costa, A.; Deyà, P. M.; Frontera, A.; Gomila, R. M.; Hunter, C. A. *J. Am. Chem. Soc.* **2006**, *128*, 5560. (b) Baldini, L.; Ballester, P.; Casnati, A.; Gomila, R. M.; Hunter, C. A.; Sansone, F.; Ungaro, R. *J. Am. Chem. Soc.* **2003**, *125*, 14181.

(25) UV-vis titrations were analyzed by fitting the whole series of spectra at 0.5 nm intervals using the software SPECIFIT. The SPECIFIT program analyzes equilibrium data sets using singular value decomposition and linear regression modeling by the Levenberg-Marquardt method to determine cumulative binding constant. (a) Gampp, H.; Maeder, M.; Meyer, C. J.; Zuberbühler, A. D. *Talanta* **1986**, *33*, 943.

(26) (a) Flamigni, L.; Talarico, A. M.; Ventura, B.; Rein, R.; Solladié, N. *Chem.—Eur. J.* **2006**, *12*, 701 and reference therein. (b) Schuster, D. I.; Li, K.; Guldi, D. M.; Ramey, J. *Org. Lett.* **2004**, *6*, 1919. (c) Brettar, J.; Gisselbrecht, J.-P.; Gross, M.; Solladié, N. *Chem. Commun.* **2001**, 733.

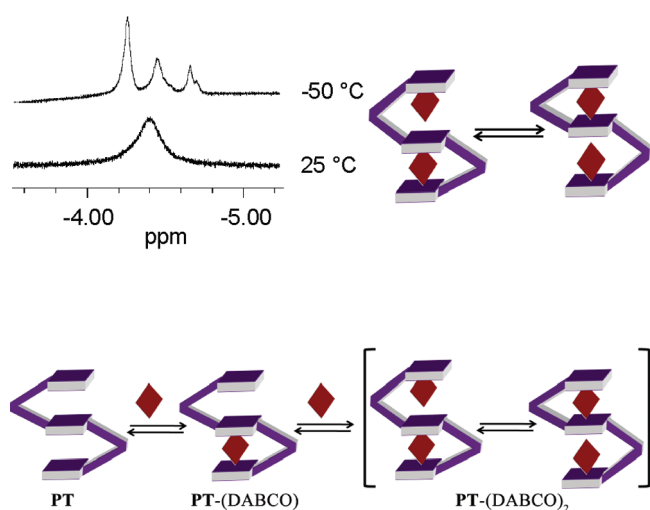


FIGURE 7. (Top Left) ^1H NMR pattern of the DABCO signal for $\text{PT}-(\text{DABCO})_2$ (0.36 mM) species at $-50\text{ }^\circ\text{C}$ in CD_2Cl_2 . (Top Right) Rapid movement of DABCO molecules in the cavity. (Bottom) Cartoon representation of the reaction of **PT** with 1 or 2 equiv of DABCO.

signals coalesced into a broad signal, advocating that now a double sandwich had formed. Subsequent addition of DABCO gradually shifted the signal further downfield until no more distinct peak was observed at $\text{PT}/\text{DABCO} = 1:3$. The peak at $\delta \approx -4.50$ ppm with a 1:2 ratio of **PT** and DABCO clearly excluded any attachment of the second DABCO toward the outside of the double cavity since a peak at $\delta \approx -3.00$ ppm is expected for a prototypical binary complex^{14a} of a zinc(II) porphyrin and DABCO.

As before, the sandwich complex was confirmed by a 3 nm red shift of the Soret and Q-band upon addition of 2 equiv of DABCO. Extra addition of DABCO resulted in a bathochromic shift of the Soret band. Further evidence for the formation of $\text{PT}-(\text{DABCO})_2$ was inferred from UV-vis titrations and a UV-vis Job plot, both showing the clean transformation of **PT** to $\text{PT}-(\text{DABCO})_2$ (Figure 6). The K_{assoc} values for $\text{PT}-(\text{DABCO})_2$ ²⁵ were evaluated as $6.3 \times 10^8 \text{ M}^{-1}$ ($\log K_1 = 8.8 \pm 0.7$) and $2.5 \times 10^{13} \text{ M}^{-2}$ ($\log \beta = 13.4 \pm 0.8$). The small K_2 value of $4.0 \times 10^4 \text{ M}^{-1}$ is in full agreement with the NMR data (peak broadening) as ligand association at the sixth binding site of the central zinc(II) porphyrin destabilizes the binding of the fifth ligand and vice versa. $\log K_1$ agrees well with $\log K$ for $\text{PD}-(\text{DABCO})$. The high value of K_1 and the small K_2 value suggest that $\text{PT}-(\text{DABCO})$ is the exclusive species formed in presence of 1 equiv of DABCO, leaving one cavity empty for a second guest molecule. This assumption is corroborated by ^1H NMR data. When 1.5 equiv of DABCO was added to **PT**, the DABCO signals were neither completely broadened nor well-separated into two singlets. Rather, the spectra response appeared like an overlap of the spectra of $\text{PT}-(\text{DABCO})$ and $\text{PT}-(\text{DABCO})_2$. Hence, the appearance of two nicely resolved singlets at $\text{PT}/\text{DABCO} = 1:1$ indicates the exclusive formation of a $\text{PT}-(\text{DABCO})$ species with one empty cavity.

Further insight was obtained upon probing $\text{PT}-(\text{DABCO})_2$ at $-50\text{ }^\circ\text{C}$ by ^1H NMR. As three singlets appeared at ~ -4.2 to -4.6 ppm (ratio 1:1:2), we postulate a scenario as depicted in Figure 7. Accordingly, altogether three nitrogen centers of the two DABCO molecules are coordinated to the three

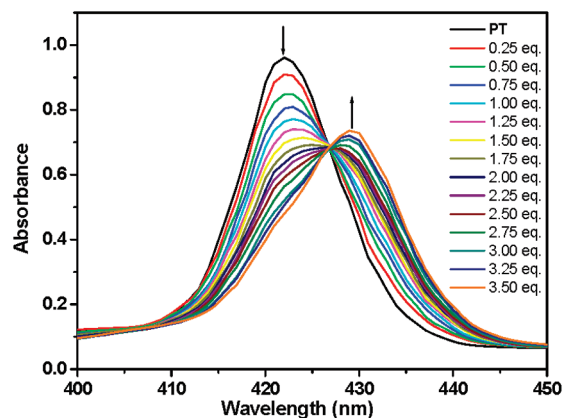
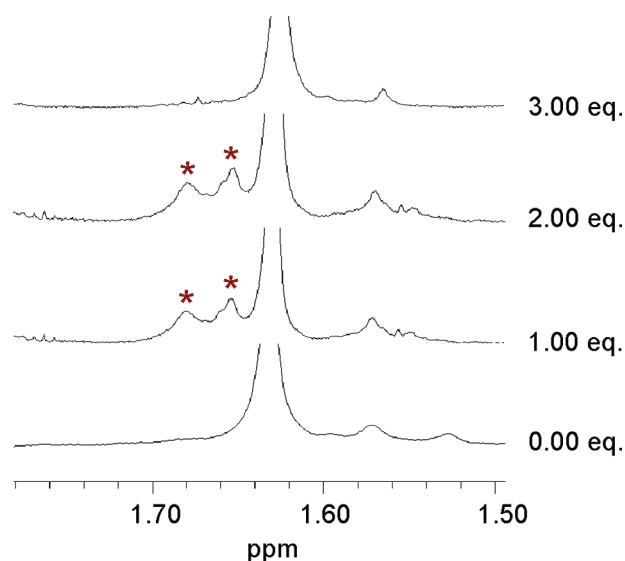


FIGURE 8. ^1H NMR titration of **PT** (0.50 mM) with pyrazine in CD_2Cl_2 at $25\text{ }^\circ\text{C}$. (Bottom) UV-vis titration of **PT** (1.20 μM) with pyrazine in CH_2Cl_2 at $25\text{ }^\circ\text{C}$ (* corresponds to the pyrazine protons).

Zn porphyrins at a given time, while the fourth nitrogen is “unbound” because a stable sixth coordination at the central Zn(II) porphyrin is impossible to achieve in solution state. Due to the three different environments, three signals are seen for the DABCO methylene protons. Those closer to the two peripheral porphyrins show up downfield, whereas the DABCO protons closer to the central porphyrin are the most upfield shifted ones. At any time, one of the DABCOs is not coordinated to the central porphyrin; its protons though are still in the shielding region of **3**, showing up as the middle signal. At room temperature, all signals merge to a broad peak, indicating that the central zinc porphyrin rapidly changes its coordination,^{4f} binding either to the top or to the bottom DABCO (Figure 7).

UV-vis titration of **PT** with pyrazine (py) resulted in a red shift of the Soret band by 4 nm upon addition of 2 equiv of py along with formation of an isosbestic point at 426 nm. Additional amounts of py led to a further bathochromic shift of the Soret band by 4 nm to 430 nm (Figure 8). A Job plot analysis indicated the formation of $\text{PT}-(\text{py})_2$. Association constants for $\text{PT}-(\text{py})_2$ ²⁵ were determined by UV-vis titration to $2.5 \times 10^6 \text{ M}^{-1}$ ($\log K_1 = 6.4 \pm 0.3$) and $5.0 \times 10^{10} \text{ M}^{-2}$ ($\log \beta = 10.7 \pm 0.3$) with $K_2 = 2.0 \times 10^4 \text{ M}^{-1}$. Notably,

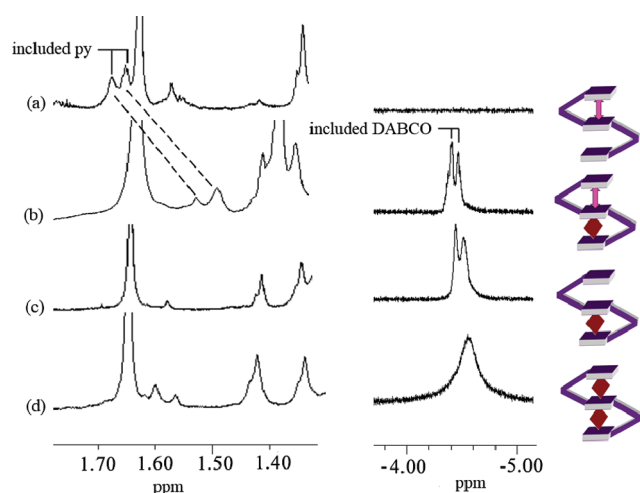


FIGURE 9. ^1H NMR spectra of mixtures of **PT**, DABCO, and pyrazine at molar ratios of (a) 1:0:1, (b) 1:1:1, (c) 1:1:0, and (d) 1:2:0 in CD_2Cl_2 .

for pyrazine binding, $\log K_2$ is $0.67 \log K_1$, whereas for binding of DABCO $\log K_2$ is only $0.52 \log K_1$. In the ^1H NMR, a 1:1 mixture of **PT** and py showed two singlets at 1.66 and 1.68 ppm corresponding to the pyrazine protons sandwiched between two porphyrins.^{26c,27} Upon addition of a further 1 equiv of py to a 1:1 mixture of **PT** and py, the two singlets remained at 1.66 and 1.68 ppm but were shifted downfield upon addition of another 1 equiv of py (Figure 8). The formation of two sharp singlets after addition of 2 equiv of pyrazine to **PT** along with above K_{assoc} values tentatively suggests that both pyrazines in **PT**-(py)₂ bind simultaneously to the central zinc(II) porphyrin unit, a feature not observed for DABCO.

As stated above, a 1:1 mixture of **PT** and DABCO led to the formation of **PT**-(DABCO). Upon addition of 1 equiv of py to **PT**-(DABCO), two singlets appeared at 1.55 ppm (for py) along with two singlets at -4.47 ppm (for DABCO) (Figure 9), confirming the formation of **PT**-(DABCO)(py). The enlarged upfield shift of the pyrazine protons as compared to that in **PT**-(py)₂ suggests a stronger binding of the pyrazine to the central porphyrin in **PT**-(DABCO)(py). Reciprocally, the same assembly was furnished when 1 equiv of DABCO was added to a 1:1 mixture of **PT** and py. The association constant of **PT**-(DABCO) with py was determined as $2.5 \times 10^5 \text{ M}^{-1}$ ($\log K = 5.4 \pm 0.3$), which is 12.5 times greater than K_2 for **PT**-(py)₂. Notably, **PT**-(DABCO)(py) was equally furnished when 1 equiv of DABCO was added to a 1:1 mixture of **PT** and py, thus allowing us to evaluate the binding of DABCO to **PT**-(py).²⁸ Here, K_{assoc} was found to be $4.0 \times 10^6 \text{ M}^{-1}$ ($\log K = 6.6 \pm 0.4$), which is 99.5 times greater than K_2 for **PT**-(DABCO)₂, again confirming the greater stability of the heteroloated species.

The increased stability of the heteroloated system may easily be understood on the basis of the different donor/acceptor qualities of DABCO and py. Whereas DABCO is only a strong σ donor, py may potentially also act as an acceptor due to

its low-lying vacant π^* orbital.²⁹ While in **PT**-(py)₂, both pyrazines compete with each other for charge transfer from the central Zn(II) porphyrin into their π^* orbitals, in **PT**-(DABCO)(py), charge transfer from the central porphyrin to py provides an extra binding for the py. In this setting, DABCO and py are electronically complementary to each other, with DABCO transmitting charge via the central porphyrin^{29,30} to the py ligand.

The present work so far illustrated a stepwise protocol to the five-component **PT**-(DABCO)(py) assembly via four orthogonal interactions,^{1f,4} and thus an orthogonal actuation of **PT**. Importantly, the five-component self-assembled aggregate was equally afforded by mixing all of the components together in $\text{CH}_3\text{CN}/\text{CH}_2\text{Cl}_2$ (3:1) and refluxing them for 4 days. Formation of **PT**-(DABCO)(py) was confirmed by ^1H NMR being exactly the same as that obtained in the stepwise approach.

Conclusion

In conclusion, we report a facile synthetic procedure to assemble the slipped cofacial porphyrin trimer **PT** that may serve as a subunit for an oligoporphyrin accordion. The two porphyrin cavities of **PT** were loaded by either two DABCOs or pyrazines and heteroloated by DABCO/pyrazine. Due to the lower stability in the former two cases and greater stability in the mixed **PT**-(DABCO)(py) system, the heteroloated double tweezer was the preferred product. Its formation is reminiscent of positive allosteric control. Furthermore, the clean one-pot synthesis of the five-component system demonstrates that all four binding interactions act in an orthogonal manner, driving the system into a single supramolecular assembly under thermodynamic equilibrium conditions.

Both the homo- and heteroloated **PT** do change incrementally the opening about the individual tweezer units that may be utilized for nanomechanical actuation, in particular with an oligoporphyrin accordion (Figure 1). Indeed, computations indicate an expansion of **PT**, as measured by the zinc–zinc distance of the lateral porphyrin units, by 2.1 Å upon addition of DABCO. Obviously, in an oligomeric porphyrin accordion with 10 **PT** subunits, the elongation upon loading would then readily rise into the 2 nm region.

Experimental Section

General Methods. Commercially available reagents were used without further purification. The solvents were dried with the appropriate desiccants and distilled prior to use. Thin-layer chromatography was performed using silica gel TLC plates. Silica gel 60 was used for column chromatography. ^1H and ^{13}C NMR spectra were recorded on 400 and 600 MHz spectrometers using the deuterated solvent as the lock and residual solvent as internal reference. The following abbreviations were utilized to describe NMR peak patterns: br s = broad singlet, s = singlet, d = doublet, t = triplet, m = multiplet. The following abbreviations were used to describe the peak patterns of IR spectra: s = sharp, m = medium, w = weak. The numbering of the carbon skeleton of the molecular formulas shown in the

(27) (a) Noworyta, K.; Marczak, R.; Tylanda, R.; Sobczak, J. W.; Chitta, R.; Kutner, W.; DSouza, F. *Langmuir* **2007**, *23*, 2555. (b) Rein, R.; Gross, M.; Solladié, N. *Chem. Commun.* **2004**, 1992. (c) Kuroda, Y.; Kawashima, A.; Hayashi, Y.; Ogoshi, H. *J. Am. Chem. Soc.* **1997**, *119*, 4929.

(28) Due to the smaller negative cooperativity in **PT**-(py)₂, a 1:1 mixture of **PT** and py produces **PT**-(py) along with some amounts of **PT**-(py)₂ and free **PT**.

(29) (a) Neyhart, G. A.; Timpson, C. J.; Bates, W. D.; Meyer, T. J. *J. Am. Chem. Soc.* **1996**, *118*, 3730. (b) Richter, M.; Brewer, K. J. *Inorg. Chem.* **1992**, *31*, 1594.

(30) (a) Hosseini, A.; Taylor, S.; Accorsi, G.; Armaroli, N.; Reed, C. A.; Boyd, P. D. W. *J. Am. Chem. Soc.* **2006**, *128*, 15903. (b) Konarev, D.; Litvinov, A. L.; Neretin, I. S.; Drichko, N. V.; Slovokhotov, Y. L.; Lyubovskaya, R. N.; Howard, J. A. K.; Yufit, D. S. *Cryst. Growth Des.* **2004**, *4*, 643. (c) Marvaud, V.; Launay, J.-P. *Inorg. Chem.* **1993**, *32*, 1376.

Experimental Section does not comply with the IUPAC nomenclature rules; it is only used for assignments of the NMR signal. Melting points were measured and are uncorrected. Binding constants were determined using the SPECFIT/32 global analysis system by Spectrum Software Associates (Marlborough, MA).²⁵ The energy-minimized structure was obtained using the MM⁺ force field as implemented in Hyperchem 7.52.

Zinc(II)-5-[4-(4'-ethynyl-2,2':6,2''-terpyridine)phenyl]-10,15,20-tris(2,4,6-trimethylphenyl)porphyrin (1). Zinc(II)-5-(4-iodophenyl)-10,15,20-tris(2,4,6-trimethylphenyl)porphyrin (**4**) (210 mg, 0.226 mmol) and 4'-ethynyl-2,2':6,2''-terpyridine (**5**) (50.0 mg, 0.194 mmol) were poured into a three-necked round-bottomed flask. Then, Pd(PPh₃)₄ (11.2 mg, 9.69 μ mol) was added to the reaction mixture. Dry NEt₃ (10 mL) and dry DMF (30 mL) were added to the reaction mixture under N₂ atmosphere. The reaction mixture was then allowed to stir at 90 °C for 12 h. The reaction mixture was evaporated to dryness, dissolved in DCM (50 mL), and washed with water (3 \times 50 mL). After drying over anhydrous Na₂SO₄, the solvent was evaporated and the residue was purified by column chromatography (SiO₂, DCM/EtOAc = 5:95). The compound was further purified over biobeads SX-3 sampling the second band in toluene: yield 62%; mp > 300 °C; ¹H NMR (400 MHz, CDCl₃) δ = 1.80 (s, 18 H, j-H), 2.63 (s, 9 H, l-H), 7.27 (s, 6 H, k-H), 7.40 (ddd, ³J = 8.4 Hz, ³J = 6.4 Hz, ⁴J = 1.2 Hz, 2 H, d-H), 7.92 (td, ³J = 8.4 Hz, ⁴J = 2.0 Hz, 2 H, e-H), 7.95 (d, ³J = 8.0 Hz, 2 H, i-H), 8.19 (d, ³J = 8.0 Hz, 2 H, h-H), 8.64 (s, 4 H, β -H), 8.69 (d, ³J = 8.4 Hz, 2 H, f-H), 8.70 (d, ³J = 4.8 Hz, 2 H, β -H), 8.74 (s, 2 H, g-H), 8.78 (m, 2 H, c-H), 8.80 (d, ³J = 4.8 Hz, 2 H, β -H) ppm; ¹³C NMR (100 MHz, CDCl₃) δ = 21.4, 21.6, 83.3, 93.8, 118.8, 119.5, 120.8, 121.2, 123.4, 124.0, 127.6, 131.0, 132.0, 132.3, 135.6, 135.8, 136.0, 137.0, 137.5, 138.8, 139.1, 142.2, 149.1, 149.2, 149.6, 149.8, 150.0, 150.1, 150.4, 155.3, 155.4 ppm; IR (KBr) ν = 3447 (br, H₂O), 2916 (m), 2361 (s), 1583 (s), 1567 (s), 1466 (m), 1391 (s), 1336 (s), 1203 (s), 1062 (s), 995 (s), 792 (s), 722 (s) cm⁻¹; ESI-MS (*m/z*) (%) 1058.4 (100), [M + H]⁺. Anal. Calcd for C₇₀H₅₃N₇Zn · 1.5H₂O: C, 77.37; H, 5.38; N, 9.02. Found: C, 77.32; H, 5.60; N, 9.34.

Zinc(II)-5-[4-[2-(4-ethynyl-2,3,5,6-tetramethylphenyl)-9-(2,4,6-trimethylphenyl)-[1,10]-phenanthroline]phenyl]-10,15,20-tris(2,4,6-trimethylphenyl)porphyrin (2). A similar procedure to that for the preparation of **1** was followed by reacting **4** (250 mg, 0.269 mmol) and **6** (83.9 mg, 0.185 mmol) with Pd(PPh₃)₄ (21.3 mg, 18.4 μ mol). The compound was purified by column chromatography (SiO₂, DCM/EtOAc = 4:96) and by size exclusion chromatography over biobeads SX-3 (second moving band in toluene): yield 59%; mp > 300 °C; ¹H NMR (400 MHz, CDCl₃) δ = 1.83 (s, 18 H, l'-H), 2.07 (s, 6 H, l2-H), 2.16 (s, 6 H, l0-H), 2.34 (s, 3 H, l1-H), 2.64 (s, 9 H, 3'-H), 2.69 (s, 6 H, l3-H), 6.97 (s, 2 H, 9-H), 7.28 (s, 6 H, 2'-H), 7.60 (d, ³J = 8.0 Hz, 1 H, 7-H), 7.61 (d, ³J = 8.0 Hz, 1 H, 4-H), 7.90 (s, 2 H, 5-, 6-H), 7.95 (d, ³J = 8.0 Hz, 2 H, b-H), 8.20 (d, ³J = 8.0 Hz, 2 H, a-H), 8.32 (d, ³J = 8.0 Hz, 1 H, 8-H), 8.35 (d, ³J = 8.0 Hz, 1 H, 3-H), 8.68 (s, 4 H, β -H), 8.75 (d, ³J = 4.8 Hz, 2 H, β -H), 8.89 (d, ³J = 4.8 Hz, 2 H, β -H) ppm; ¹³C NMR (100 MHz, CDCl₃) δ = 17.8, 18.6, 20.6, 21.1, 21.5, 21.7, 21.8, 90.0, 97.0, 118.5, 118.7, 119.2, 123.1, 123.3, 125.0 (2C), 126.2, 126.4, 127.2, 127.6, 128.5, 129.5, 130.6, 131.0, 131.1, 131.9, 132.1, 132.3, 134.4, 135.8, 135.9, 136.2, 136.3, 137.3, 137.5, 138.1, 139.1 (2C), 139.2, 141.5, 142.8, 146.2, 149.6, 149.7, 149.8 (2C), 160.3, 161.2 ppm; IR (KBr) ν = 2916 (br), 2358 (br), 1578 (s), 1562 (s), 1465 (m), 1391 (m), 1325 (w), 1190 (m), 1062 (m), 995 (s), 865 (m), 792 (s) cm⁻¹; ESI-MS (*m/z*) (%) 1255.6 (100), [M + H]⁺. Anal. Calcd for C₈₆H₇₄N₆Zn · CH₃CO₂C₂H₅: C, 80.37; H, 6.14; N, 6.25. Found: C, 79.87; H, 5.98; N, 6.55.

Zinc(II)-5,15-bis[4-[2-(4-ethynyl-2,3,5,6-tetramethylphenyl)-9-(2,4,6-trimethylphenyl)-[1,10]-phenanthroline]phenyl]-10,20-bis(2,4,6-trimethylphenyl)porphyrin (3). Precursors **7** (50.0 mg, 49.3 μ mol) and **6** (48.0 mg, 0.106 mmol) with Pd(PPh₃)₄ (10.0 mg, 8.66 μ mol) were reacted according to the procedure for **1**. The compound was purified by column chromatography (SiO₂,

hexane/EtOAc = 85:15) and by size exclusion chromatography over biobeads SX-3 isolating the first moving band in toluene: yield 55%; mp > 300 °C; ¹H NMR (400 MHz, CDCl₃) δ = 1.85 (s, 12 H, l'-H), 2.06 (s, 12 H, l2-H), 2.15 (s, 12 H, l0-H), 2.33 (s, 6 H, l1-H), 2.65 (s, 6 H, 3'-H), 2.68 (s, 12 H, l3-H), 6.96 (s, 4 H, 9-H), 7.30 (s, 4 H, 2'-H), 7.59 (d, ³J = 8.4 Hz, 2 H, 7-H), 7.60 (d, ³J = 8.4 Hz, 2 H, 4-H), 7.90 (s, 4 H, 5-, 6-H), 7.96 (d, ³J = 8.4 Hz, 4 H, b-H), 8.25 (d, ³J = 8.4 Hz, 4 H, a-H), 8.32 (d, ³J = 8.4 Hz, 2 H, 8-H), 8.35 (d, ³J = 8.4 Hz, 2 H, 3-H), 8.81 (d, ³J = 4.8 Hz, 4 H, β -H), 8.95 (d, ³J = 4.8 Hz, 4 H, β -H) ppm; ¹³C NMR (100 MHz, CDCl₃) δ = 17.9, 18.6, 20.6, 21.1, 21.5, 21.7, 90.1, 97.0, 119.5, 119.7, 123.2, 123.3 (2C), 125.0, 125.1, 126.2, 126.4, 127.2, 127.7, 128.5, 129.6, 130.9, 132.2 (2C), 134.5, 135.8, 135.9, 136.2, 136.3, 137.4, 137.5, 138.2, 139.0, 139.2, 141.6, 142.5, 146.3 (2C), 149.9, 150.0, 160.3, 161.2 ppm; IR (KBr) ν = 2947 (w), 2916 (s), 2855 (w), 2360 (w), 2343 (w), 1609 (w), 1586 (s), 1490 (s), 1436 (w), 1377 (w), 1336 (w), 1204 (s), 1099 (w), 1064 (w), 998 (s), 884 (w), 851 (s), 798 (s) cm⁻¹; ESI-MS (*m/z*) (%) 1666.8 (100), [M + H]⁺. Anal. Calcd for C₁₁₆H₉₆N₈Zn · 2H₂O: C, 81.79; H, 5.92; N, 6.58. Found: C, 81.57; H, 6.26; N, 6.34.

Complex PD. In an NMR tube, **2** (2.98 mg, 2.37 μ mol) and Zn(OTf)₂ (0.862 mg, 2.37 μ mol) were dissolved in deuterated acetonitrile/dichloromethane (3:1) and heated for 2 h at 60 °C. Then **1** (2.51 mg, 2.37 μ mol) was added to the solution, which was heated at 60 °C for 3 h to afford **PD** in quantitative yield: mp > 300 °C; ¹H NMR (400 MHz, CD₃CN/CD₂Cl₂ = 3:1) δ = 1.15 (s, 6 H, mes-H), 1.20 (s, 6 H, mes-H), 1.23 (s, 6 H, mes-H), 1.31 (s, 12 H, mes-H), 1.51 (s, 6 H, mes-H), 1.69 (s, 6 H, mes-H), 1.81 (s, 3 H, mes-H), 1.84 (s, 3 H, mes-H), 1.98 (s, 3 H, mes-H), 2.05 (s, 6 H, duryl-H), 2.33 (s, 6 H, duryl-H), 2.46 (s, 6 H, mes-H), 2.51 (s, 3 H, mes-H), 2.57 (s, 3 H, mes-H), 6.33 (s, 2 H, 9-H), 6.85 (s, 3 H, [2' or K]-H), 7.00 (s, 3 H, [2' or K]-H), 7.16 (s, 2 H, [2' or K]-H), 7.25 (s, 2 H, [2' or K]-H), 7.30 (s, 2 H, [2' or K]-H), 7.59 (ddd, ³J = 7.4 Hz, ³J = 5.2 Hz, ⁴J = 0.8 Hz, 2 H, d-H), 7.80 (m, 2 H, c-H), 8.05 (d, ³J = 8.0 Hz, 2 H, i-H), 8.12 (d, ³J = 8.0 Hz, 2 H, b-H), 8.17 (d, ³J = 4.4 Hz, 2 H, β -H), 8.20 (d, ³J = 8.0 Hz, 2 H, h-H), 8.24 (d, ³J = 4.4 Hz, 2 H, β -H), 8.27 (d, ³J = 8.0 Hz, 2 H, a-H), 8.32 (d, ³J = 4.4 Hz, 2 H, β -H), 8.34 (d, ³J = 4.4 Hz, 2 H, β -H), 8.40 (dt, ³J = 7.4 Hz, ⁴J = 1.6 Hz, 2 H, e-H), 8.44 (d, ³J = 4.4 Hz, 4 H, β -H), 8.45 (br s, 2 H, [4,7]-H), 8.48 (d, ³J = 4.4 Hz, 2 H, β -H), 8.60 (s, 2 H, 5-, 6-H), 8.66 (d, ³J = 7.4 Hz, 2 H, f-H), 8.82 (s, 2 H, g-H), 8.84 (d, ³J = 4.4 Hz, 2 H, β -H), 9.17 (d, ³J = 8.0 Hz, 1 H, [3 or 8]-H), 9.21 (d, ³J = 8.0 Hz, 1 H, [3 or 8]-H) ppm; IR (KBr) ν = 2921 (s), 2200 (s), 1601 (s), 1478 (s), 1277 (s), 1259 (s), 1030 (s), 996 (s), 797 (m), 638 (s) cm⁻¹; ESI-MS (*m/z*) (%) 1190.6 (100), [M - 2OTf]²⁺. Anal. Calcd for C₁₅₈H₁₂₉F₆N₁₃O₆S₂Zn₃ · CH₂Cl₂: C, 69.07; H, 4.78; N, 6.59; S, 2.32. Found: C, 68.67; H, 4.87; N, 6.21; S, 2.36.

Complex PT. Compound **3** (3.45 mg, 2.07 μ mol) and Zn(OTf)₂ (1.50 mg, 4.14 μ mol) were added to a round-bottomed flask, dissolved in deuterated acetonitrile/dichloromethane (3:1) and heated for 2 h at 60 °C. Then **1** (4.39 mg, 4.14 μ mol) was added to the solution, and heating at 60 °C was continued for 4 h to furnish **PT** in quantitative yield: mp > 300 °C; ¹H NMR (400 MHz, CD₃CN) δ = 0.63 (s, 9 H, mes-H), 1.09 (s, 15 H, mes-H), 1.11 (s, 15 H, mes-H), 1.20 (s, 12 H, mes-H), 1.59 (s, 9 H, mes-H), 1.82 (s, 9 H, mes-H), 1.90 (s, 6 H, mes-H), 2.03 (s, 12 H, duryl-H), 2.09 (s, 6 H, mes-H), 2.36 (s, 12 H, duryl-H), 2.50 (s, 6 H, mes-H), 2.60 (s, 3 H, mes-H), 6.30 (s, 4 H, 9-H), 6.55 (s, 4 H, [2' or k]-H), 6.84 (s, 6 H, [2' or k]-H), 7.19 (s, 4 H, [2' or k]-H), 7.33 (s, 2 H, [2' or k]-H), 7.58 (t, ³J = 7.0 Hz, 4 H, d-H), 7.65 (d, ³J = 8.0 Hz, 4 H, i-H), 7.80 (d, ³J = 8.0 Hz, 4 H, b-H), 7.82 (m, 4 H, c-H), 7.91 (d, ³J = 8.0 Hz, 4 H, a-H), 8.03 (d, ³J = 8.0 Hz, 4 H, h-H), 8.07 (d, ³J = 4.4 Hz, 4 H, β -H), 8.16 (d, ³J = 4.4 Hz, 4 H, β -H), 8.18 (d, ³J = 4.4 Hz, 4 H, β -H), 8.23 (d, ³J = 8.0 Hz, 2 H, [4 or 7]-H), 8.27 (d, ³J = 8.0 Hz, 2 H, [4 or 7]-H), 8.34 (d, ³J = 4.4 Hz, 4 H, β -H), 8.37 (t, ³J = 7.0 Hz, 4 H, e-H), 8.55 (d, ³J = 4.4 Hz, 4 H, β -H), 8.60 (d, ³J = 4.4 Hz, 4 H, β -H), 8.61 (s, 4 H, 5-, 6-H), 8.64

(d, $^3J = 7.0$ Hz, 4 H, f-H), 8.80 (s, 4 H, g-H), 9.19 (d, $^3J = 8.0$ Hz, 2 H, [3 or 8]-H), 9.22 (d, $^3J = 8.0$ Hz, 2 H, [3 or 8]-H) ppm; IR (KBr) $\nu = 2921$ (s), 2853 (s), 2214 (br), 2200 (br), 1611 (s), 1601 (s), 1478 (s), 1376 (w), 1336 (w), 1276 (w), 1258 (s), 1224 (w), 1203 (w), 1153 (s), 1062 (w), 1030 (s), 996 (s), 852 (w), 797 (s), 722 (w), 638 (s) cm^{-1} ; ESI-MS m/z (%) = 979.4 (100) $[\text{M} - 4\text{OTf}]^{4+}$, 1355.5 (55) $[\text{M} - 3\text{OTf}]^{3+}$. Anal. Calcd for $\text{C}_{260}\text{H}_{206}\text{F}_{12}\text{N}_{22}\text{O}_{12}\text{-S}_4\text{Zn}_5\cdot 3\text{CH}_2\text{Cl}_2$: C, 66.24; H, 4.48; N, 6.46; S, 2.69. Found: C, 66.52; H, 4.97; N, 6.11; S, 2.35.

Acknowledgment. Financial support by Deutsche Forschungsgemeinschaft and the University of Siegen is gratefully acknowledged.

Supporting Information Available: ^1H NMR, ^{13}C NMR, ESI-MS, UV-vis, and DOSY discussed for all relevant compounds and tweezers. This material is available free of charge via the Internet at <http://pubs.acs.org>.